

## Temperature Dependence of the Deuterium Quadrupole Coupling Constants and the Correlation Times for Neat Formamide

Mary J. Hansen, Mark A. Wendt, and Thomas C. Farrar\*

Department of Chemistry, University of Wisconsin—Madison, 1101 University Avenue, Madison, Wisconsin 53706

Received: January 4, 2000; In Final Form: March 20, 2000

High-level ab initio calculations yield a linear relationship between the proton chemical shift,  $\delta_{\text{H}}$ , and the deuterium quadrupole coupling constant,  $\chi_{\text{D}}$ , for the amide protons in neat, liquid formamide. An experimental measurement of  $\delta_{\text{H}}$  in combination with the linear relationships provides an accurate value for  $\chi_{\text{D}}$  in the hydrogen-bonded liquid; subsequent measurements of the deuterium relaxation rate provide a means to obtain effective rotational correlation times in the neat liquid. Temperature-dependent proton chemical shifts and relaxation rates for the three nuclei in formamide are presented. The chemical shift data and the ab initio calculations indicate that both amide protons hydrogen bond, whereas the C–H proton does not participate in hydrogen bonding in the neat liquid. The effective correlation times at room temperature were found to be 9.2 ps for the trans N–D vector, 6.3 ps for the cis N–D vector, and 5.2 ps for the C–D vector. This indicates that in the neat liquid formamide rotates anisotropically.

### Introduction

Hydrogen bonding plays a central role in the structure of many important molecules such as proteins. The peptide groups within a protein form intramolecular N–H $\cdots$ O=C hydrogen bonds which determine the secondary structure of the protein.<sup>1</sup> Formamide is an interesting and important molecule for study because it is the smallest unit in a peptide chain and is often selected to model the bonding in peptides. Although tremendous effort has been made to characterize the hydrogen bonding present in liquid formamide, a detailed picture of the supramolecular structure that agrees with both theory and experiment remains an elusive goal.

The structure of formamide in the solid state is known to consist of long zigzag chains cross-linked by hydrogen bonds that form a network of molecules;<sup>2</sup> the gas phase consists of monomers.<sup>3</sup> Experimental liquid-state studies such as ESCA,<sup>4</sup> vibrational spectroscopy,<sup>5–12</sup> NMR,<sup>13–15</sup> and diffraction experiments<sup>16–21</sup> have produced inconsistent models of the liquid structure. The structures suggested include linear chains,<sup>10,11,15,16,20</sup> cyclic clusters,<sup>14,18,21</sup> and branched clusters.<sup>12,17</sup> These inconsistencies arise because the experimental results are difficult to interpret. Raman and IR data primarily consist of rather broad featureless peaks; therefore, specific structural information is quite limited. Liquid-state NMR chemical shift data generally consist of sharp lines, but the NMR time scale is slow and one obtains information only about the time-averaged chemical environment; information about individual clusters is absent. X-ray and neutron diffraction experiments provide information about pair correlation functions which are related to hydrogen bond lengths but are not sensitive to the supramolecular structure. The final result is that none of the experimental data provide a clear, unique picture of the liquid structure.

Many molecular dynamics (MD) and Monte Carlo (MC) simulations have been performed on formamide and have

produced varying results. A MC simulation by Jorgensen and Swenson<sup>22</sup> and a MD simulation by Sagarik and Ahlrichs<sup>23</sup> both concluded that although a cyclic formamide dimer is more energetically favored, linear chainlike clusters dominate the liquid structure due to entropy effects. A later MD study by Puhovski and Rode<sup>24</sup> concluded again that the cyclic dimer is favored energetically, but "... liquid formamide consists of a continuous H-bond network with a minor number of small clusters not included in this network" and that "... chain-like associates are also not dominating the H-bond network." In contrast to both of the previous results, a recent MC study by Cordeiro<sup>25</sup> concludes that liquid formamide primarily consists of cyclic dimers.

Other theoretical studies have given varying results as well. Torii and Tasumi<sup>26</sup> calculated the vibrational spectra of both linear and branched clusters of formamide and compared the spectra to experimental results. They concluded that the hydrogen bonding in liquid formamide is two-dimensional. They go on to say that the spectral features "... cannot be reproduced by formation of a one-dimensional hydrogen bond chain alone." A new model for liquids employs quantum statistical mechanics to calculate populations of clusters.<sup>27</sup> This model called quantum cluster equilibrium (QCE) concluded that the structure of liquid formamide mainly consists of cyclic hexamers<sup>28</sup> with minimal intercluster interactions; this result does not agree with NMR proton chemical shift data reported here. Neither the simulations nor the current models for liquids are able to give a complete picture of liquid formamide. At the present time there is no consensus on the structure of liquid formamide.

The proton isotropic chemical shift,  $\delta_{\text{H}}$ , contains information about hydrogen bonding in the gas, liquid, or solid state. Experimental chemical shift studies of hydrogen-bonded liquids have shown that as hydrogen bonding increases, the chemical shift frequencies of the participating protons increase (e.g. see Liddel and Ramsey<sup>29</sup>). For example, the chemical shift of the trans amide proton in gas phase formamide is 4.79 ppm,<sup>30</sup> and

\* To whom correspondence should be addressed. E-mail: tfarrar@chem.wisc.edu. Fax: (608) 262-9918.

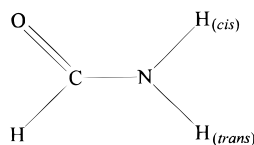


**Figure 1.** Labeling of the formamide protons.

the chemical shift for the same proton in the neat liquid is 7.65 ppm<sup>31</sup> (see Figure 1 for the labeling of the formamide protons).

A number of studies have used quadrupole coupling constants to monitor the extent of hydrogen bonding.<sup>32–35</sup> The quadrupole coupling constant,  $\chi_Q$ , is defined in units of Hertz as

$$\chi_Q = \frac{e^2 q_{zz} Q}{h} \quad (1)$$

where  $Q$  is the nuclear quadrupole moment (a quantity known with reasonable accuracy<sup>36</sup>),  $q_{zz}$  is the principle component of the electric field gradient tensor,  $e$  is the electronic charge, and  $h$  is Planck's constant. Because the electric field gradient at the nucleus is dependent on hydrogen bonding, the quadrupole coupling constant,  $\chi_Q$ , is sensitive to hydrogen bonding. The deuterium quadrupole coupling constant,  $\chi_D$ , is especially sensitive to hydrogen bonding. The term quadrupole coupling constant is a misnomer because it is now known that  $\chi_Q$  values can vary significantly with temperature, solvent, concentration, and physical state.<sup>13,37,38</sup> For example  $\chi_D$  in solid D<sub>2</sub>O is 213 kHz,<sup>39</sup> whereas in the gas phase it is 308 kHz.<sup>40</sup> The change in hydrogen bonding is the generally accepted explanation for this difference in the two coupling constants.

In 1980, Berglund and Vaughan<sup>41</sup> investigated hydrogen bonding in solids and found correlations between proton chemical shift tensors, deuterium quadrupole coupling constant values, and hydrogen bond distances. On the basis of this early work, theoretical correlations between these parameters have been investigated for liquid methanol.<sup>38</sup> With electronic structure packages such as Gaussian 98,<sup>42</sup> calculations of electric field gradients and chemical shielding tensors have become accurate and routine. With the electric field gradients, quadrupole coupling constants can be calculated using eq 1. Similarly, with chemical shielding tensors, isotropic chemical shifts can be calculated (one-third the trace of the chemical shift tensor). A theoretical linear relationship between  $\chi_D$  and  $\delta_H$  provides an indirect method to experimentally determine  $\chi_D$ .  $\delta_H$  is a parameter that can be easily and accurately measured and may be used as a reliable way to obtain accurate values for  $\chi_D$  in the hydrogen-bonded liquid.

$\chi_D$  is related to the deuterium relaxation rate,  $R_1$ , and the molecular correlation time,  $\tau_c$ , by the equation<sup>43</sup>

$$R_1 = \frac{1}{T_1} = \frac{3\pi^2}{10} \chi_D^2 \left( 1 + \frac{\eta^2}{3} \right) \left\{ \frac{\tau_c}{1 + \omega_o^2 \tau_c^2} + \frac{4\tau_c}{1 + 4\omega_o^2 \tau_c^2} \right\} \quad (2)$$

where  $\eta$  is the asymmetry parameter and  $\omega_o$  is the Larmor frequency. The asymmetry parameter for deuterium is usually quite small ( $\leq 0.2$ ) and the  $\eta^2/3$  term may be dropped from the calculation. If  $\chi_D$  is known, a measurement of  $R_1$  provides a value for  $\tau_c$ . Because the quadrupolar relaxation mechanism is more than 2 orders of magnitude larger than other relaxation mechanisms (e.g. dipolar or chemical shift anisotropy), these other relaxation processes may be neglected. In the extreme narrowing region where  $\omega_o \tau_c \ll 1$ , eq 2 reduces to

$$R_1 = \frac{1}{T_1} = \frac{3\pi^2}{2} \chi_D^2 \tau_c \quad (3)$$

Equations 2 and 3 assume that the rotations obey a Brownian diffusion process and that the molecular reorientation can be described by a single correlation time. For asymmetric top molecules, such as formamide, this assumption may not be valid. In this case, relaxation data and quadrupole coupling constants for three nonequivalent quadrupolar nuclei within the molecule are necessary to determine the three components of the rotational diffusion tensor. The applicability of this equation to liquid formamide is discussed further in the Results and Discussion section.

Spin–lattice relaxation rates and chemical shifts are directly measurable quantities. Using an ab initio correlation between  $\chi_D$  and  $\delta_H$ , indirect experimental values for  $\chi_D$  may be readily found. An effective  $\tau_c$  for the X–D (X = C or N) vectors can then be calculated using eq 3 and the experimental values for  $R_1$ . In this study, we report temperature-dependent proton chemical shifts and deuterium spin–lattice relaxation rates for neat, liquid formamide. We also report a linear relationship between the ab initio  $\delta_H$  and ab initio  $\chi_D$  for 15 different formamide clusters. From these data, experimental  $\chi_D$  and effective  $\tau_c$  values may be calculated for all of the deuterium nuclei.

The question of whether liquid formamide rotates isotropically or anisotropically has been the focus of many studies. In some of these studies values for the quadrupole coupling constants were taken from the solid or gas phase. However, as was mentioned above for water, the quadrupole coupling constants in the liquid and solid phase can differ drastically. Therefore, the conclusion on how formamide rotates in the liquid depends heavily on the values used for the quadrupole coupling constants as this term is squared in eq 2. In this study, the quadrupole coupling constants are semiempirical values measured in the liquid state and have been found to depend on temperature, as would be expected from changes in hydrogen bonding. By using this new method of measuring the quadrupole coupling constant in the liquid, the isotropic or anisotropic nature of the rotation in formamide can be determined.

## Experimental Methods

The <sup>2</sup>H and <sup>1</sup>H NMR spectra were recorded on a home-built spectrometer operating at 7.00 T using a 5 mm probe. The magnet is an eighth-order corrected solenoid manufactured by Cryomagnet Systems. The magnet and its environment are sufficiently stable that no internal lock is necessary for periods up to several hours. The high-temperature data were collected by passing nitrogen gas over a heater and then around the sample. The lower temperature data were collected by passing the nitrogen gas through either an ethanol–dry ice bath or an ice water bath and across the heater to the sample. The temperatures were calibrated using Van Geet's<sup>44</sup> relationship for the chemical shift difference in methanol,  $\Delta\delta_M$ :

$$T(\text{K}) = 402.99 - 29.46\Delta\delta_M - 23.83\Delta\delta_M^2 \quad (4)$$

This temperature dependence is well characterized for the temperature range of  $175 \leq T \leq 330$  K. The temperature measurements are accurate to  $\pm 0.05$  K.

Formamide (99.5+%, Aldrich), formamide-*d*<sub>3</sub> (98%, Cambridge Isotope Laboratories, Inc.), and tetramethylsilane (99.9%, Cambridge Isotope Laboratories, Inc.) were used without further purification. All sample tubes were cleaned with nitric acid,

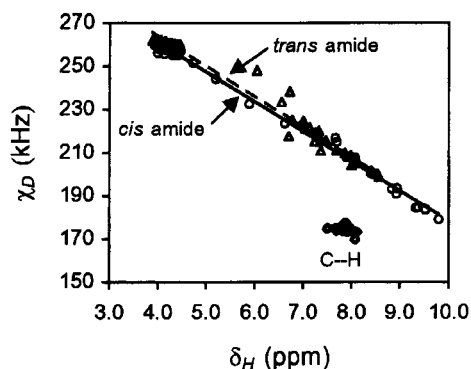


**Figure 2.** Theoretical relationship for the dependence of  $\chi_D$  on the chemical shift. Ab initio calculations were performed at the B3LYP/6-31+G\* level of theory. The cis proton is represented by  $\circ$ , trans by  $\triangle$ , and C-H by  $\diamond$ . The dashed line corresponds to the least-squares best fit for the trans amide proton calculations; the solid line corresponds to the best fit for the cis amide proton.

followed by EDTA to remove any trace metals. The tubes were then rinsed with deionized water and dried in vacuo for at least 24 h before use. The formamide- $d_3$  sample was thoroughly degassed using several freeze-pump-thaw cycles on a high vacuum line. The formamide sample used for the chemical shift measurements included a capillary of tetramethylsilane as an external reference. The spin-lattice relaxation rates for formamide were measured using an inversion recovery pulse sequence experiment using an average  $180^\circ$  pulse width of 55  $\mu$ s. The spin-lattice relaxation rates were reproducible to  $\pm 3\%$ .

## Results and Discussion

**Theoretical Results.** Ab initio calculations were performed on 15 different clusters of formamide using the Gaussian 98 and Gaussian 94 electronic structure programs.<sup>42,45</sup> The clusters vary in size from monomer to hexamer with a wide range of geometries including linear, cyclic, and formations based on amide crystal structures. The hydrogen bonds in the formamide clusters were of the type N-H $\cdots$ O. No hydrogen bonds to the C-H or to the nitrogen were considered. All calculations were performed at the B3LYP/6-31+G\* level of theory. Electric field gradients and isotropic chemical shielding values for these clusters were calculated using the optimized geometry at the same level of theory. To convert these results to quadrupole coupling constants and chemical shift values, a value of 2.860 mb was used for the deuterium nuclear quadrupole moment<sup>36</sup> and a value of 31.8 ppm was used for the chemical shielding of TMS. The value for the chemical shielding of TMS was calculated at the B3LYP/6-31+G\* level of theory.

The linear relationship between calculated quadrupole coupling constants and calculated chemical shifts is shown in Figure 2. The individual points on this graph correspond to individual calculations for each of the protons within a monomer unit of a cluster. For a hexamer of formamide molecules each monomer within the cluster contributes 1 point for cis amide, trans amide, and C-H nuclides for a total of 18 points in Figure 2. The C-H chemical shift and C-D quadrupole coupling constant remained essentially invariant for the different clusters. This result is not surprising because none of the clusters considered hydrogen bonding to the C-H. The calculations for the cis amide proton revealed a linear relationship between  $\chi_D$  and  $\delta_H$  and least-squares analysis ( $R^2 = 0.99$ ) of the data produced the following relation:

$$\chi_D \text{ (kHz)} = 315 - 13.6\delta_H \text{ (ppm)} \quad (5)$$

**TABLE 1: Proton Chemical Shifts,  $\delta_H$ , and Deuterium Quadrupole Coupling Constants,  $\chi_D$ , as a Function of Temperature for Neat, Liquid Formamide**

$T$ (K)	$\delta_H$ (ppm)			$\chi_D$ (kHz)		
	trans	cis	C-H	trans	cis	C-D
262	7.60	7.42	7.98	214	214	175
266	7.57	7.38	7.98	214	215	175
269	7.54	7.35	7.97	214	215	175
273	7.52	7.32	7.97	215	215	175
277	7.49	7.30	7.96	215	216	175
280	7.47	7.27	7.96	215	216	175
286	7.43	7.23	7.95	216	217	175
292	7.40	7.19	7.95	216	217	175
299	7.36	7.15	7.95	217	218	175
305	7.33	7.12	7.95	217	218	175
310	7.30	7.09	7.95	218	219	175
316	7.27	7.06	7.95	218	219	175
323	7.24	7.03	7.96	219	220	175
328	7.22	7.01	7.96	219	220	175
333	7.20	6.99	7.97	219	220	175

Similarly, the trans amide proton displayed the linear relationship ( $R^2 = 0.98$ )

$$\chi_D \text{ (kHz)} = 322 - 14.2\delta_H \text{ (ppm)} \quad (6)$$

The chemical shift calculations performed to generate eqs 5 and 6 were calculated using the GIAO method.<sup>46</sup> To check their validity, the values for the gas-phase proton chemical shift values ( $\delta_H(\text{cis}) = \delta_H(\text{trans}) = 4.79 \text{ ppm}^{30}$ ) were compared to the calculated values for the monomer,  $\delta_H(\text{cis}) = 4.04 \text{ ppm}$  and  $\delta_H(\text{trans}) = 3.88 \text{ ppm}$ . The experimental gas phase measurements were taken at high temperature, and so only one chemical shift is observed due to rapid rotation about the C-N bond. Unfortunately, solid-phase proton chemical shifts for formamide have not been measured; however, a comparison of the calculated chemical shifts for a hydrogen-bonded cluster and low-temperature experimental proton chemical shifts may be made. In this case, the proton chemical shifts at 260 K (Table 1) are 7.42 ppm for the cis amide proton and 7.60 ppm for the trans amide proton. The average calculated chemical shift for a formamide cyclic cluster with cis amide proton hydrogen bonds and for a cyclic cluster with trans amide proton hydrogen bonds is about 8.5 ppm. These comparisons between the calculated and experimental chemical shifts show that the calculations exhibit the correct trend, if not the absolute value, of shift to higher frequency for stronger hydrogen bonding.

The average  $\chi_D$  for the amide deuterons of solid formamide has been measured to be  $195.0 \pm 0.1 \text{ kHz}$ ,<sup>45</sup> however, the gas phase  $\chi_D$  value is not reported in the literature. By substitution of the available experimental data into eqs 5 and 6, specific trends can be identified. The gas-phase chemical shift listed above generates  $\chi_D$  values of 250 and 254 kHz for the cis and trans amide deuterons, respectively. Similarly, using the low-temperature chemical shift values listed above and eqs 5 and 6, a value of 214 kHz was calculated for both the cis and trans amide deuterons, close to the solid-state value. This trend of decreasing  $\chi_D$  with decreasing temperature has been found for many systems of small molecules that hydrogen bond such as methanol<sup>38</sup> and water.<sup>39,40</sup>

**Experimental Results.** The chemical shifts of the three formamide protons were measured at various temperatures in the range 260–330 K and are shown in Figure 3; the formamide protons are labeled as shown in Figure 1. The spectral assignment of the amide proton peaks was based on  $^{15}\text{N}$ -formamide NMR measurements by Sunners et al.<sup>48</sup> This assignment places the trans amide proton peak at a higher



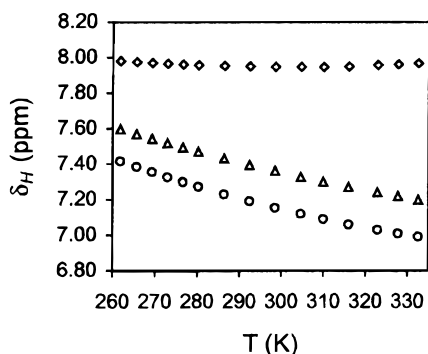


**Figure 3.** Temperature dependence of the experimental proton chemical shifts for the cis proton  $\circ$ , trans proton  $\Delta$ , and C–H  $\diamond$  in neat, liquid formamide.

frequency than the cis amide proton for the neat liquid. This result is based on the well-known assumption that  $J_{HH}$  spin-coupling constants from protons at a  $180^\circ$  dihedral angle are larger than couplings from  $0^\circ$  dihedral angles.<sup>49,50</sup>

Table 1 summarizes the temperature-dependent  $\delta_H$  values as well as the semiempirical  $\chi_D$  values using eqs 5 and 6. The average  $\chi_D$  value from the ab initio calculations for the C–D deuteron is  $175 \text{ kHz} \pm 4\%$  (Table 1), which agrees well with the experimental value of  $180 \text{ kHz}$  for a deuteron bonded to an  $sp^2$ -hybridized carbon.<sup>51</sup> As can be seen from Figure 3, as temperature increases the amide proton frequencies shift to lower values whereas the C–H proton frequency remains unchanged. As discussed above, the shift to lower frequency at higher temperature for the amide protons indicates weaker hydrogen bonding. As temperature increases, both the trans amide proton and the cis amide proton shift to lower frequency at the same rate. Therefore, the shift to lower frequency going from the cold, liquid phase to the gas phase is about equal for both the cis (2.4 ppm) and trans (2.6 ppm) amide protons. The ab initio calculations also indicate that the cis and trans amide protons experience nearly equal changes in chemical shift in going from the monomer, gas-phase environment to the hydrogen-bonded liquid phase. Thus both theory and experiment indicate substantial hydrogen bonding to both amide protons in the liquid. In contrast to the amide protons, the  $\delta_H$  value for the C–H proton does not change significantly with temperature, indicating that the C–H proton does not participate in the hydrogen bonding in liquid formamide.

The observation that both amide protons are equally involved in the hydrogen bonding in liquid formamide brings up interesting questions concerning some cluster models present in the literature. One cluster model proposes that at room temperature 95% of liquid formamide is present as a cyclic hexamer with trans amide hydrogen bonds and the other 5% consists of linear tetramers also with trans hydrogen bonds.<sup>14</sup> This model indicates that a negligible amount of the cis amide protons are hydrogen bonded. The experimental temperature-dependent data presented here indicate that this model is not correct. Similarly, a cluster model of mainly cyclic dimers has been proposed and suggests mainly cis hydrogen bonds and minimal trans hydrogen bonds;<sup>18</sup> this type of model does not agree with the chemical shift data.

The deuterium relaxation rates were measured in the temperature range 250–370 K. The data are presented in Figure 4 and also in Table 2. At most temperatures two distinct signals are seen for the amide deuterons due to hindered rotation about the C–N axis. At high temperatures the deuterium chemical shifts coalesce due to the rapid rotation about the C–N bond. At low temperatures the spin–spin relaxation rates,  $R_2$ , for the

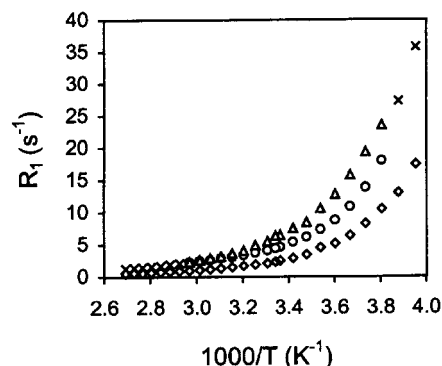


**Figure 4.** Temperature dependence of the experimental relaxation rates for the cis deuteron  $\circ$ , trans deuteron  $\Delta$ , C–D  $\diamond$ , and amide deuterons  $\times$ .

**TABLE 2: Temperature Dependence of the Formamide Deuterium Relaxation Rates,  $R_1$ , for Neat, Liquid Formamide**

$T$ (K)	$R_1$ ( $s^{-1}$ )			$T$ (K)	$R_1$ ( $s^{-1}$ )		
	trans	cis	C–D		trans	cis	C–D
253	35.7	35.7	17.4	312	4.12	3.33	1.73
259	27.2	27.2	13.0	317	3.66	3.06	1.52
263	23.5	17.9	10.5	322	3.19	2.88	1.32
268	19.4	13.8	8.22	327	2.92	2.56	1.20
273	15.8	10.8	6.41	332	2.59	2.46	1.10
278	12.8	8.72	5.13	336	2.32	2.26	0.998
283	10.6	7.29	4.52	342	2.11	2.11	0.932
287	8.44	6.14	3.47	347	1.94	1.94	0.849
292	7.52	5.36	2.90	352	1.68	1.68	0.771
297	6.47	4.60	2.54	357	1.62	1.62	0.694
299	6.39	4.42	2.34	362	1.50	1.50	0.629
302	5.53	4.09	2.10	366	1.42	1.42	0.602
307	4.90	3.74	1.90	371	1.30	1.30	0.561

amide deuterons become quite large due to scalar relaxation via the spin-coupled  $^{14}\text{N}$  nucleus. This leads to very broad line widths and loss of spectral resolution. Data for the deuterium relaxation rates have been previously reported in the literature.<sup>13</sup> Calculations performed on the relaxation data from ref 13 indicate that the peak assignment placed the cis deuteron at higher frequency than the trans deuteron, opposite from the spectral assignment used in this work. The discrepancy in the relaxation data presented here and that of ref 13 is rooted only in the amide peak assignment. The C–D relaxation rates from ref 13 are in excellent agreement with the data presented here.

From the measured proton chemical shifts and eqs 5 and 6,  $\chi_D$  can be obtained for all of the formamide deuterons. With the measured relaxation rates and the semiempirical  $\chi_D$  values, eq 3 can be used to calculate temperature-dependent effective correlation times (summarized in Table 3). The temperature dependence of the correlation times is shown in Figure 5. The temperature dependence is given approximately by the Arrhenius relation,

$$\tau_c = \tau_0 e^{E_a/RT} \quad (7)$$

The expected trend of decreasing correlation time with increasing temperature is observed. The activation energies for molecular reorientation,  $E_a$ , were found to be 23.7, 21.0, and 23.5 kJ/mol for the trans N–D, cis N–D, and C–D vectors, respectively. The preexponential factors,  $\tau_0$ , were found to be 0.64, 1.5, and 0.43 fs for the trans N–D, cis N–D, and C–D vectors, respectively. At room temperature, the effective correlation time for the trans N–D vector is 9.2 ps. This value is almost a factor of 2 longer than the effective correlation times

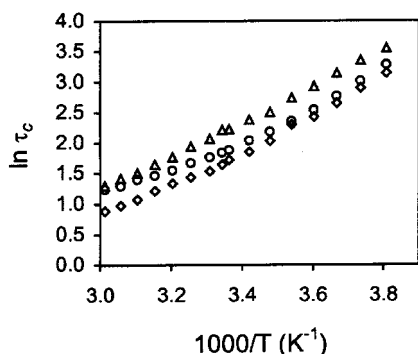


**Figure 5.** Arrhenius plot of the effective correlation times for the cis N–D vector  $\circ$ , trans N–D vector  $\Delta$ , and C–D vector  $\diamond$  in neat, liquid formamide.

**TABLE 3: Effective Correlation Times,  $\tau_c$ , and Viscosities,  $\eta$ , as a Function of Temperature for Neat, Liquid Formamide**

$T$ (K)	$\tau_c$ (ps)			$\eta$ (cP)
	trans N–D	cis N–D	C–D	
263	34.8	26.4	23.1	10.42
268	28.5	20.2	18.1	8.61
273	23.1	15.8	14.1	7.24
278	18.6	12.6	11.3	6.14
283	15.4	10.5	10.0	5.25
287	12.2	8.8	7.6	4.52
292	10.8	7.7	6.4	3.92
297	9.3	6.6	5.6	3.42
299	9.2	6.3	5.2	3.26
302	7.9	5.8	4.6	3.00
307	7.0	5.3	4.2	2.65
312	5.9	4.7	3.8	2.35
317	5.2	4.3	3.4	2.10
322	4.5	4.0	2.9	1.88
327	4.1	3.6	2.6	1.69
332	3.6	3.4	2.4	1.53

for the cis N–D vector at 6.3 ps and the C–D vector at 5.2 ps. The value of 5.2 ps for the C–D vector is in good agreement with other reported values of 5.0 ps for the C–D vector<sup>52</sup> and 5.0 ps for the  $^{13}\text{C}$ –H vector.<sup>13</sup>

The longer effective correlation time for the trans N–D vector at temperatures below 300 K (for which there is no appreciable internal motion) may be attributed to a large amplitude, librational motion about the trans amide H–N–C=O axis, assigned in the low-frequency Raman spectrum at  $195\text{ cm}^{-1}$ .<sup>11</sup> The motion about this axis would not affect the correlation time for the trans N–D vector, which is on-axis, but would shorten the correlation times for the cis N–D and C–D vectors, which are off-axis. If this was the only intramolecular motion present, the correlation times for both the cis N–D and C–D vectors would be the same; however they differ by 20%. Hence, there must be an additional motion affecting the C–D vector correlation time but not the cis N–D vector correlation time. Hydrogen bonding to the cis amide proton would hinder the range of motions possible. Because the C–H is not hydrogen bonded, as indicated by the chemical shift data, its motion is not hindered and leads to a shorter correlation time.

The effective correlation times of all the X–D ( $X = \text{C}$  or  $\text{N}$ ) vectors and the temperature-dependent viscosity data are presented in Table 3. These effective correlation times may also provide information about cluster size and shape. The Stokes–Einstein–Debye (SED) model<sup>53–55</sup> has been shown to give reasonable cluster volumes for hydrogen-bonded systems such as neat methanol and methanol in carbon tetrachloride.<sup>38</sup> On the basis of these previous studies, it was tempting to calculate

cluster volumes for neat formamide and compare the results with available experimental data. The SED model relates the correlation time to the volume of the solute providing insight into the size of the clusters. However, the SED relation gives correlation times that are 5 or 6 times longer than expected because SED models the solute as a sphere rotating in a solvent of infinitely small spheres. Gierer and Wirtz<sup>56</sup> (GW) developed a microviscosity factor,  $f$ , which is a function of the size and shape of the solute molecule relative to the solvent ( $0 \leq f \leq 1$ ) to correct this oversimplification. The SED relation using the GW microviscosity factor is

$$\tau_c = f \frac{V\eta}{kT} \quad (8)$$

where  $V$  is the volume of the rotating species,  $\eta$  is the viscosity of the solution,  $k$  is Boltzmann's constant, and  $T$  is the temperature. A detailed description of how to calculate the volumes using the SED equation is given in refs 38, 57, and 58. Using the SED equation, volumes for differently shaped clusters were calculated using trans amide effective correlation times and experimental viscosity data.<sup>59</sup> The trans amide correlation times are the longest and, therefore, most likely to represent the overall motions of any clusters present. The room-temperature SED volumes from eq 8 were then compared to volumes calculated using the ESURF algorithm.<sup>60</sup> The ESURF algorithm estimates the volume of a cluster by enclosing each atom of the optimized structure in a sphere of empirical van der Waals radius<sup>61</sup> to form a space-filling model. The only cluster that shows good agreement between the ESURF volume and the SED volume is the cyclic dimer (all cis hydrogen bonds). Therefore, the SED relation predicts that neat formamide primarily consists of cyclic dimers.

As mentioned above, a simple model of cyclic dimers does not agree with other literature data. Given the chemical shift data reported here along with the other experimental data cited above, it is clear that both amide protons in formamide experience significant hydrogen bonding and not just the cis amide protons. The discrepancy between the chemical shift data and the SED predicted cluster volumes may arise in several ways. The high-frequency chemical shift of the trans amide proton can be attributed to the formation of chains of cyclic dimers similar to what is found in the crystal structure of formamide. The SED volume size of dimers may then be attributed to dimer lifetimes that are long compared to the NMR correlation time with chain segment lifetimes shorter than the NMR correlation time. Another explanation may be that the effective correlation time for the trans amide vector used to calculate the SED volumes is not representative of the overall cluster motion in the liquid. If local motions are present, such as the large-amplitude librational motion mentioned above, then the trans N–D correlation time may be more representative of these motions than the cluster motion.

Still a further explanation may be that the SED model is not valid for neat formamide. The SED model works well for aliphatic alcohols<sup>38</sup> that have small, well-defined structures and cluster lifetimes that are long compared to  $\tau_c$ . In contrast, formamide has multiple hydrogen bond donors and multiple hydrogen bond acceptors. This may give rise to a continuous network of hydrogen bonds instead of discrete clusters, which would not allow for clear definitions of species that are considered in the SED model. Since the microviscosity factor depends on the size and shape of the solute and solvent molecules, it becomes difficult if not impossible to find a meaningful value for this parameter. For these reasons we think

that the SED relation is not appropriate for formamide and possibly for other molecules with multiple hydrogen bond donors and acceptors.

A word or two should be said about the applicability of eq 2 to neat formamide. Equation 2 is derived by assuming that the rotations obey a Brownian diffusion process and that the molecular reorientation can be described by a single correlation time. The validity of using the diffusion model for formamide can be tested by comparing the correlation time with the free rotor time,  $\tau_f$ . The free rotor time is described by

$$\tau_f = \left( \frac{I_{av}}{kT} \right)^{1/2} \quad (9)$$

where  $I_{av}$  is the average moment of inertia,  $k$  is Boltzmann's constant, and  $T$  is the temperature. If the correlation time for the liquid is long compared to  $\tau_f$ , then the diffusion model is sufficient to describe the reorientation in the liquid.<sup>63</sup> For a single formamide molecule optimized at B3LYP/6-31+G\*,  $\tau_f$  is 0.40 ps at 260 K and 0.35 ps at 330 K. Since the effective correlation times calculated for the liquid are over a factor of 10 greater than the free rotor time for the temperatures of interest, the reorientation in the liquid can be described using a diffusion model.

As mentioned, eq 2 also assumes that a single correlation time describes the reorientation of a molecule. For deuterons that lie on the symmetry axis of an asymmetric top, e.g.  $\text{CDCl}_3$ , a single correlation time is sufficient to describe the motion and eq 2 is valid. Because multiple studies in the literature<sup>13,52,62</sup> have concluded isotropic or nearly isotropic motion for liquid formamide, eq 2 should be appropriate producing only a single correlation time. In this study, however, it is clear that the three geometrically different vectors have three different effective correlation times. Formamide is an asymmetric top, and the diagonal elements of the rotational diffusion tensor are different. To completely determine these different components, the formalism described in detail for quadrupolar relaxation of an asymmetric top by Huntress<sup>63</sup> and Woessner<sup>64</sup> should be followed. Since there are three nonequivalent quadrupolar nuclei in formamide- $d_3$ , one can obtain all three diagonal elements of the rotational diffusion tensor. The correlation times obtained in this study for formamide are "effective" correlation times which are appropriately averaged values of the three components of the rotational diffusion tensor. The final result is that formamide rotates anisotropically.

## Conclusions

High-level ab initio calculations show that the quadrupole coupling constants for the amide deuterons in formamide are linearly related to the proton isotropic chemical shift ( $R^2 = 0.99$  and 0.98). Consequently, a measurement of the temperature-dependent chemical shifts in the neat liquid provides reliable, semiempirical values for the temperature-dependent deuterium quadrupole coupling constants. The temperature-dependent chemical shifts indicate that both the cis and trans amide protons contribute about equally to the hydrogen bonding present in liquid formamide. The quadrupole coupling constant for C–D remains constant at a value of 175 kHz in sharp contrast to the amide deuteron quadrupole coupling constants that change significantly with temperature. A value for the quadrupole coupling constant provides temperature-dependent effective molecular correlation times that range from 35 ps at 260 K to 3 ps at 330 K. The effective molecular correlation times at room temperature were found to be 9.2 ps for the trans N–D vector,

6.3 ps for the cis N–D vector, and 5.2 ps for the C–D vector clearly indicating that the motion in neat, liquid formamide is anisotropic.

**Acknowledgment.** We thank the National Science Foundation, Grant No. CHE-9500735, for the support of this research. M.H. and M.W. thank the National Science Foundation for financial support.

## References and Notes

- (1) Jeffrey, G. A. *An Introduction to Hydrogen Bonding*; Oxford University Press: New York, 1997.
- (2) Ladell, J.; Post, B. *Acta Crystallogr.* **1954**, *7*, 559.
- (3) King, S. T. *J. Phys. Chem.* **1971**, *75*, 405.
- (4) Siegbahn, H.; Asplund, L.; Kelfve, P.; Hamrin, K.; Karlsson, L.; Siegbahn, K. *J. Electron Spectrosc. Relat. Phenom.* **1974**, *5*, 1059.
- (5) Lee, Y. *J. Raman Spectrosc.* **1997**, *28*, 45.
- (6) Nielsen, O. F.; Mortensen, A.; Yarwood, J.; Shelley, V. *J. Mol. Struct.* **1995**, *378*, 1.
- (7) Mortensen, A.; Nielsen, O. F.; Yarwood, J.; Shelley, V. *J. Phys. Chem.* **1994**, *98*, 5221.
- (8) Mortensen, A.; Nielsen, O. F.; Yarwood, J.; Shelley, V. *J. Phys. Chem.* **1995**, *99*, 4435.
- (9) Goossens, K.; Smeller, L.; Heremans, K. *J. Chem. Phys.* **1993**, *99*, 5736.
- (10) Nielsen, O. F.; Christensen, D. H.; Rasmussen, O. H. *J. Mol. Struct.* **1991**, *242*, 273.
- (11) Nielsen, O. F.; Lund, P. A.; Praestgaard, E. *J. Chem. Phys.* **1982**, *77*, 3878.
- (12) Gardiner, D. J.; Lees, A. J.; Straughan, B. P. *J. Mol. Struct.* **1979**, *52*, 15.
- (13) Ludwig, R.; Bohmann, J.; Farrar, T. C. *J. Phys. Chem.* **1995**, *99*, 9681.
- (14) Ludwig, R.; Weinhold, F.; Farrar, T. C. *J. Chem. Phys.* **1995**, *102*, 5118.
- (15) Hippler, M.; Hertz, H. G. *Z. Phys. Chem.* **1992**, *75*, 25.
- (16) Bellissent-Funel, M.; Nasr, S.; Bosio, L. *J. Chem. Phys.* **1997**, *106*, 7913.
- (17) DeSando, R. J.; Brown, G. H. *J. Phys. Chem.* **1968**, *72*, 1088.
- (18) Wiesmann, F. J.; Zeidler, M. D.; Bertagnolli, H.; Chieux, P. *Mol. Phys.* **1986**, *57*, 275.
- (19) Kálmán, E.; Serke, I.; Pálkás, G.; Zeidler, M. D.; Wiesmann, F. J.; Bertagnolli, H.; Chieux, P. *Z. Naturforsch.* **1983**, *38A*, 231.
- (20) Ohtaki, H.; Funaki, A.; Rode, B. M.; Reibnegger, G. *J. Bull. Chem. Soc. Jpn.* **1983**, *56*, 2116.
- (21) Miyake, M.; Kaji, O.; Nakagawa, N.; Suzuki, T. *J. Chem. Soc., Faraday Trans. 2* **1985**, *81*, 277.
- (22) Jorgensen, W. L.; Swenson, C. J. *J. Am. Chem. Soc.* **1985**, *107*, 569.
- (23) Sagarik, K. P.; Ahlrichs, R. *J. Chem. Phys.* **1987**, *86*, 5117.
- (24) Puhovski, Y. P.; Rode, B. M. *Chem. Phys.* **1995**, *190*, 61.
- (25) Marques Cordeiro, J. M. *Int. J. Quantum Chem.* **1997**, *65*, 709.
- (26) Torii, H.; Tasumi, M. *Int. J. Quantum Chem.* **1998**, *70*, 241.
- (27) Weinhold, F. *J. Chem. Phys.* **1998**, *109*, 367.
- (28) Ludwig, R.; Weinhold, F.; Farrar, T. C. *J. Chem. Phys.* **1995**, *103*, 3636.
- (29) Liddel, U.; Ramsey, N. F. *J. Chem. Phys.* **1951**, *19*, 1608.
- (30) Vaara, J.; Kaski, J.; Jokisaari, J.; Diehl, P. *J. Phys. Chem.* **1997**, *101A*, 5069. The proton chemical shifts for the gas phase were referenced by  $^{13}\text{C}$ -methane. To convert the chemical shifts to be referenced by TMS a factor of 31.03 ppm was used.
- (31) Sørensen, O. W.; Scheibye, S.; Lawesson, S. O.; Jakobsen, H. *J. Org. Magn. Reson.* **1981**, *16*, 322.
- (32) Ludwig, R.; Farrar, T. C.; Zeidler, M. D. *J. Phys. Chem.* **1994**, *98*, 6684.
- (33) Struis, R. P. W. J.; De Bleijser, J.; Leyte, J. C. *J. Phys. Chem.* **1987**, *91*, 1639.
- (34) Ichikawa, K.; Kameda, Y.; Yamaguchi, T.; Wakita, H.; Misawa, M. *Mol. Phys.* **1991**, *73*, 79.
- (35) Reimers, J. R.; Watts, R. O. *Chem. Phys.* **1984**, *91*, 201.
- (36) Pyykkö, P. *Z. Naturforsch.* **1991**, *47A*, 189.
- (37) Stringfellow, T. C.; Farrar, T. C. *J. Chem. Phys.* **1995**, *102*, 9465.
- (38) Wendt, M.; Farrar, T. C. *Mol. Phys.* **1998**, *95*, 1077.
- (39) Waldstein, P.; Rabideau, S. W.; Jackson, J. A. *J. Chem. Phys.* **1964**, *41*, 214.
- (40) Bluysen, H.; Verhoeven, J.; Dymanus, A. *Phys. Lett.* **1967**, *25A*, 214.
- (41) Berglund, B.; Vaughan, R. W. *J. Chem. Phys.* **1980**, *73*, 2037.
- (42) Frisch, M. J.; Trucks, G. W.; Schlegel, H. B.; Scuseria, G. E.; Robb, M. A.; Cheeseman, J. R.; Zakrzewski, V. G.; Montgomery Jr., J. A.; Stratmann, R. E.; Burant, J. C.; Dapprich, S.; Millam, J. M.; Daniels, A.

- D.; Kudin, K. N.; Strain, M. C.; Farkas, O.; Tomasi, J.; Barone, V.; Cossi, M.; Cammi, R.; Mennucci, B.; Pomelli, C.; Adamo, C.; Clifford, S.; Ochterski, J.; Petersson, G. A.; Ayala, P. Y.; Cui, Q.; Morokuma, K.; Malick, D. K.; Rabuck, A. D.; Raghavachari, K.; Foresman, J. B.; Cioslowski, J.; Ortiz, J. V.; Stefanov, B. B.; Liu, G.; Liashenko, A.; Piskorz, P.; Komaromi, I.; Gomperts, R.; Martin, R. L.; Fox, D. J.; Keith, T.; Al-Laham, M. A.; Peng, C. Y.; Nanayakkara, A.; Gonzalez, C.; Challacombe, M.; Gill, P. M. W.; Johnson, B.; Chen, W.; Wong, M. W.; Andres, J. L.; Gonzalez, C.; Head-Gordon, M.; Replogle, E. S.; Pople, J. A. *Gaussian 98*, Revision A.6; Gaussian Inc.: Pittsburgh, PA, U.K., 1998.
- (43) Abragam, A. *Principles of Nuclear Magnetism*; Clarendon Press: Oxford, U.K., 1961; Chapter 8.
- (44) Van Geet, A. L. *Anal. Chem.* **1970**, *42*, 679.
- (45) Frisch, M. J.; Trucks, G. W.; Schlegel, H. B.; Gill, P. M. W.; Johnson, B. G.; Robb, M. A.; Cheeseman, J. R.; Keith, T.; Petersson, G. A.; Montgomery, J. A.; Raghavachari, K.; Al-Laham, M. A.; Zakrzewski, V. G.; Ortiz, J. V.; Foresman, J. B.; Cioslowski, J.; Stefanov, B. B.; Nanayakkara, A.; Challacombe, M.; Peng, C. Y.; Ayala, P. Y.; Chen, W.; Wong, M. W.; Andres, J. L.; Replogle, E. S.; Gomperts, R.; Martin, R. L.; Fox, D. J.; Binkley, J. S.; Defrees, D. J.; Baker, J.; Stewart, J. P.; Head-Gordon, M.; Gonzalez, C.; Pople, J. A. *Gaussian 94*, Revision E.2 (Pittsburgh, PA: Gaussian Inc.: Pittsburgh, PA, U.K., 1995).
- (46) Wolinski, K.; Hinton, J. F.; Pulay, P. *J. Am. Chem. Soc.* **1990**, *112*, 8251.
- (47) Edmonds, D. T.; Hunt, M. J.; Mackay, A. L. *J. Magn. Reson.* **1975**, *20*, 505.
- (48) Sunners, B.; Piette, L. H.; Schneider, W. G. *Can. J. Chem.* **1960**, *38*, 681.
- (49) Karplus, M. *J. Chem. Phys.* **1959**, *30*, 11.
- (50) Karplus, M. *J. Am. Chem. Soc.* **1963**, *85*, 2870.
- (51) Saitô, H.; Mantsch, H. H.; Smith, I. C. P. *J. Am. Chem. Soc.* **1973**, *95*, 8453.
- (52) Weingärtner, H.; Holz, M.; Hertz, H. G. *J. Solution Chem.* **1978**, *7*, 689.
- (53) Stokes, G. *Trans. Cambridge Philos. Soc.* **1856**, *9*, 5.
- (54) Einstein, A. *Investigations on the Theory of Brownian Movement*; Dover: New York, 1956; pp 19–34.
- (55) Debye, P. *Polar Molecules*; Dover: New York, 1929.
- (56) Gierer, A.; Wirtz, K. *Z. Naturforsch.* **1953**, *8A*, 532.
- (57) Boéré, R. T.; Kidd, R. G. Rotational Correlation Times in Nuclear Magnetic Relaxation. In *Annual Reports on NMR Spectroscopy*; Webb, G. A., Ed.; Academic Press: New York, 1982; pp 319–361.
- (58) Wendt, M. A.; Zeidler, M. D.; Farrar, T. C. *Mol. Phys.* **1999**, *97*, 753.
- (59) Taniewska-Osinska, S.; Piekarska, A.; Kacperska, A. *J. Solution Chem.* **1983**, *12*, 717.
- (60) Silla, E.; Tunon, I.; Pascual-Ahuir, J. L. *J. Comput. Chem.* **1991**, *12*, 1077.
- (61) Pauling, L. *Nature of the Chemical Bond*; Cornell University Press: Ithaca, NY, 1960; p 257 ff.
- (62) Burgar, M. I.; St. Amour, T. E.; Fiat, D. *J. Phys. Chem.* **1981**, *85*, 502.
- (63) Huntress, W. T., Jr. *J. Chem. Phys.* **1968**, *48*, 3524.
- (64) Woessner, D. E. *J. Chem. Phys.* **1962**, *37*, 647.